




3-[3-(Phenalkylamino)cyclohexyl]phenols: Synthesis, biological activity, and in silico investigation of a naltrexone-derived novel class of MOR-antagonists

Graziella Tocco¹  | Antonio Laus¹ | Maksims Vanejevs² | Anastasija Ture² |
Rafaela Mostallino³ | Nicholas Pintori³ | Maria Antonietta De Luca³  |
M. Paola Castelli³  | Gaetano Di Chiara^{3,4}

¹Department of Life and Environmental Sciences, University of Cagliari, Cittadella Universitaria di Monserrato, Monserrato, Cagliari, Italy

²Laboratory of CNS Active Compounds, Latvian Institute of Organic Chemistry, Riga, Latvia

³Department of Biomedical Sciences, University of Cagliari, Cittadella Universitaria di Monserrato, Monserrato, Cagliari, Italy

⁴Neuroscience Institute, National Research Council of Italy (CNR), Cagliari, Italy

Correspondence

Graziella Tocco, Department of Life and Environmental Sciences, University of Cagliari, Cittadella Universitaria di Monserrato, Monserrato, 09042 Cagliari, Italy.
Email: toccog@unica.it

Funding information

The European Commission under the Call JUST-2017-AGDRUG SUPPORTING INITIATIVES IN THE FIELD OF DRUGS POLICY, JUST-2017-AG-DRUG, Grant/Award Number: 806996-JUSTSO

Abstract

The development of novel μ -opioid receptor (MOR) antagonists is one of the main objectives of drug discovery and development. Based on a simplified version of the morphinan scaffold, 3-[3-(phenalkylamino)cyclohexyl]phenol analogs were designed, synthesized, and evaluated for their MOR antagonist activity in vitro and in silico. At the highest concentrations, the compounds decreased by 52% to 75% DAMGO-induced GTP γ S stimulation, suggesting that they acted as antagonists. Moreover, Extra-Precision Glide and Generalized-Born Surface Area experiments provided useful information on the nature of the ligand–receptor interactions, indicating a peculiar combination of C-1 stereochemistry and N-substitutions as feasibly essential for MOR–ligand complex stability. Interestingly, compound **9** showed the best experimental binding affinity, the highest antagonist activity, and the finest MOR–ligand complex stability. In silico experiments also revealed that the most promising stereoisomer (1R, 3R, 5S) **9** retained 1,3-*cis* configuration with phenol ring equatorial oriented. Further studies are needed to better characterize the pharmacodynamics and pharmacokinetic properties of these compounds.

KEYWORDS

[³H]DAMGO binding assay, 3-[3-(phenalkylamino)cyclohexyl]phenols, GTP γ S assay, in silico study, MOR antagonists

1 | INTRODUCTION

Despite the serious and potentially fatal adverse effects, μ -opioid receptor (MOR) agonists such as morphine, oxycodone, and fentanyl, have been over/misprescribed in recent years, resulting in a dramatic increase in opioid dependence, illegal opioid use, and opioid-related

deaths. Opioid antagonists are a class of drugs that bind competitively to one or more of the opioid receptors, present little or no intrinsic activity, and robustly antagonize the effects of receptor agonists. They are utilized as antidotes for opioid overdose (naltrexone) and approved for the treatment of opioid and alcohol dependence (naltrexone). Several structural classes have been identified as MOR antagonists with variable

M. Paola Castelli and Gaetano Di Chiara are co-senior authors.

This is an open access article under the terms of the Creative Commons Attribution License, which permits use, distribution and reproduction in any medium, provided the original work is properly cited.

© 2022 The Authors. *Archiv der Pharmazie* published by Wiley-VCH GmbH on behalf of Deutsche Pharmazeutische Gesellschaft.

degrees of selectivity for MOR, delta, and kappa opioid receptors.^[1] Naltrexone, obtained from oxymorphone by simple substitutions of cyclopropylmethyl for a methyl group, is considered a relatively pure antagonist that binds to all three opioid receptors. It has efficacy by the oral route, and long duration of action and is utilized for opioid and alcohol dependence treatment (e.g., REVIA[®], VIVITROL[®], and NALOREX[®]) as it reduces craving and euphoria associated with substance use disorder; its use is often associated with nausea, anxiety, headache, dizziness, vomiting, decreased appetite, hyperalgesia, muscle cramps, cold symptoms. Given the complexity of the substance use disorders in humans, but also other therapeutic indications linked to MOR antagonism (e.g., obesity, psychosis, and Parkinson's disease)^[2] the design of new naltrexone analogs is a pivotal goal of drug discovery and development.

During the long history of MOR-targeting drugs, researchers went, step by step, from natural opioid morphine structures to simplified ones. In this context, *N*-substituted *trans*-3,4-dimethyl-4-(3-hydroxyphenyl)-piperidines^[3,4] and 4-(3-hydroxyphenyl)piperazines^[5] represent privileged scaffolds of pure opioid antagonists. In particular, Zimmermann et al.^[3,4,6,7] pointed out the structural significance, in terms of MOR binding affinity and antagonist potency, of the 3-(piperidin-4-yl)phenol core *N*-substituted with a phenylethyl or phenylpropyl chain and on the equatorial orientation of phenol ring mandatory for antagonist activity. Analogously, Hashimoto et al. reported on the crucial impact of the *N*-phenalkyl substitution of 5-(3-hydroxyphenyl)morphanes on the MOR affinity and on receptor antagonism^[8,9] (Figure 1).

With this in mind, in the present research, exploiting naltrexone as a structural prototype and applying a simple synthetic approach, we disclosed the 3-[3-(phenalkylamino)cyclohexyl]phenol core as the starting background to design new MOR antagonists (Figure 1). In detail, we elected three crucial structural features to be present in the newly designed moieties: (1) a 3-hydroxyphenyl group, (2) an amino group substituted with a phenylethyl or phenylpropyl chain at a specified distance from the OH group, and (3) a lipophilic core structure combining these elements.

The phenylalkyl moiety has been selected as the *N*-substituent of choice, as it is present in a variety of morphans, piperidines, and other chemical scaffolds provided by MOR antagonist activity.^[3,7-10] Additionally, phenylalkyl substituent should increase lipophilicity to the rather small morphinan structure. The methyl group (R) in position 5 to the cyclohexane ring might be important as a conformation stabilizer, also affecting compound potency. In fact, its role as a modulator of MOR functional activity has already been reported for a series of *trans*-3,4-dimethyl-4-(3-hydroxyphenyl)-piperidines.^[11] To better elucidate its importance, derivatives without -CH₃ group in position 5 were also synthesized. The synthesized derivatives were tested for their ability to displace [³H]DAMGO ([D-Ala², NMe-Phe⁴, Gly-ol⁵]-enkephalin) from its binding site and evaluated for the MOR antagonist activity by guanosine 5'-O-(3-[³⁵S]thiotriphosphate (GTPγS) assay. Extra-Precision Glide (Glide-XP) and MM-GBSA in silico protocols were, then, applied to deeply

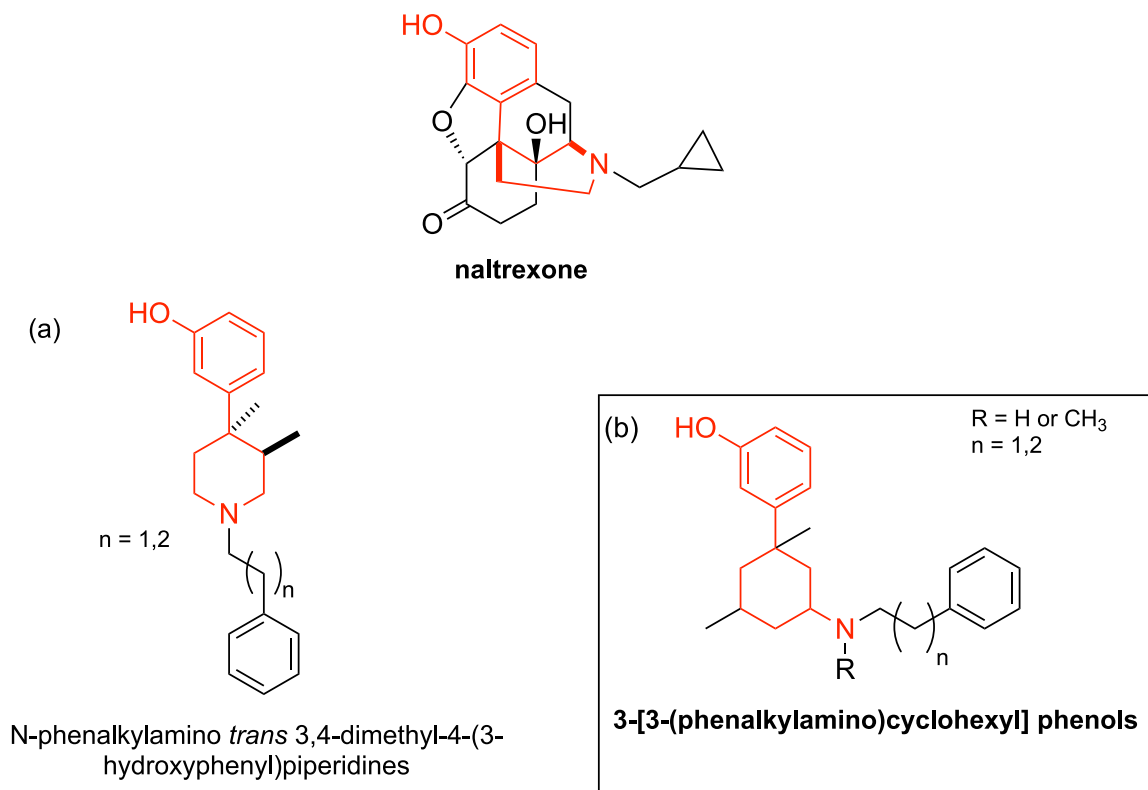


FIGURE 1 Naltrexone and chemical structures of *N*-phenalkylamino *trans* 3,4-dimethyl-4-(3-hydroxyphenyl)piperidines (a), *N*-phenalkyl 5-(3-hydroxyphenyl)morphanes (b) and 3-[3-(phenalkylamino)cyclohexyl]phenols

investigate the nature of the ligand–receptor interactions, identifying the most promising stereoisomer for each compound by virtue of the free binding energy values of the ligand–receptor complexes.

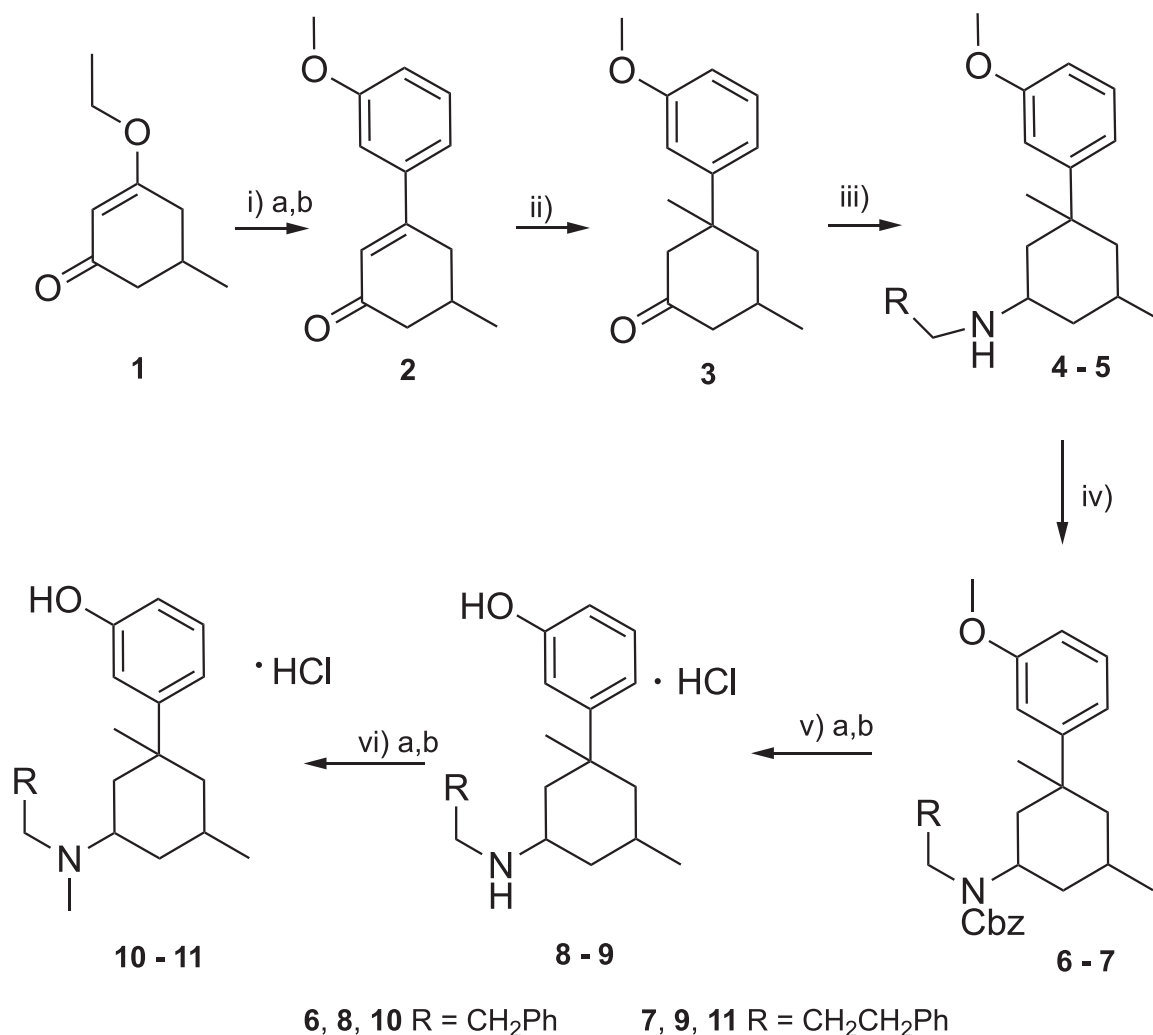
2 | RESULTS AND DISCUSSION

2.1 | Chemistry

The synthesis of 3-[3-(phenalkylamino)cyclohexyl]phenols started with the introduction of the methoxyphenyl group by the addition of 3-methoxyphenyl magnesium bromide to ketone **1**. Treatment of carbinol intermediate with aqueous hydrochloric acid gave cyclohexenone **2**. Conjugate 1,4-addition of organocuprate,^[12] generated in situ from methylmagnesium bromide to cyclohexenone **2**, afforded the required 3-(3-methoxyphenyl)-3,5-dimethylcyclohexan-1-one **3**. Further on, reductive amination of ketone **3** afforded *N*-phenalkyl-3-(3-methoxyphenyl)-3,5-dimethylcyclohexan-1-amine **4** and **5**.

Acylation of intermediates **4** and **5** with benzyl chloroformate in the presence of triethylamine has been used to ease the separation of products **6** and **7**. Cleavage of aryl methoxy group of compounds **6** and **7** by boron tribromide proceeded with concomitant removal of *N*-Cbz group, providing target amines **8** and **9**. Additionally, tertiary amines **10** and **11** have been prepared by reductive alkylation of compounds **8** and **9** respectively, with formaldehyde (Scheme 1). All the compounds were isolated as hydrochloride salts and structurally characterized by means of ¹H-NMR (nuclear magnetic resonance), ¹³C-NMR, and HRMS (high-resolution mass spectrometry) spectroscopic methods (see the Supporting Information).

The conjugated addition of 3-hydroxybenzeneboronic acid to 2-methylcyclohex-2-en-1-one **12** has been selected as an optimal approach to preparing 3-methyl-3-(3-hydroxyphenyl)cyclohexanone **13**, which served as a useful building block in the synthesis of 3-[1-methyl-3-(phenethylamino)cyclohexyl]phenol **14** and 3-[1-methyl-3-(phenylpropylamino)cyclohexyl]phenol **15**. Subsequently, the reductive amination of ketone **13** provided the final phenol derivatives **14**



SCHEME 1 Synthesis of compounds **8**, **9**, **10**, and **11**. Reagents and conditions: (i) a. 3-MeOC₆H₄MgBr, Et₂O; b. aq. HCl; (ii) MeMgBr, THF, Et₂O, cat. CuCl; (iii) corresponding primary amine, NaBH(OAc)₃, MeOH; (iv) CbzCl, Et₃N, acetonitrile; (v) a. BBr₃, CH₂Cl₂; b. 4 N HCl/Et₂O; (vi) a. (CH₂O)_n, NaBH₃CN, MeOH; b. 4 N HCl/Et₂O.

and **15**, which were isolated as hydrochloride salts by treatment with 4 N HCl in Et₂O (Scheme 2).

2.2 | Biology

The racemic 3-[3-(phenalkylamino)cyclohexyl]phenols **8**, **9**, **10**, **11**, **14**, and **15** were then tested for their ability to displace specific binding (SB) of the MOR agonist [³H]DAMGO. Specifically, [³H]DAMGO displacement experiments were carried out by using several dilutions (0.01, 0.1, 1, and 10 μM) of cold DAMGO or of compounds **8**, **9**, **10**, **11**, **14**, and **15**. Affinities at MOR for all compounds were determined by measuring their ability to displace specific [³H]DAMGO binding in a membrane preparation of rat brain (minus cerebellum). As shown in Table 1, all compounds displaced [³H]DAMGO binding in a concentration-dependent manner with varying affinities ranging from 44% to 99% (0.01–10 μM) for **9**, the compound showing the highest affinity for MOR. Indeed, **9** at a concentration of 0.1 to 10 μM displayed an affinity similar to our reference compound DAMGO. At 0.01 μM the compounds **10**, **8**, and **11** showed a similar profile, while at 0.1 μM were able to displace [³H]DAMGO from its binding site, with the rank order of **9** > **10** ≈ **8** > **11**. Compounds **14** and **15** were almost ineffective.

Subsequently, to determine their potential ability as MOR antagonists, functional characterization of the synthesized compounds was performed using the GTPγS binding assay, a well-validated functional assay for G protein-coupled receptors,^[13] using membranes from rat brain cortex. To assay for MOR antagonist activity, the compounds were tested in the presence of MOR agonist, DAMGO (10 μM). Under our experimental conditions, the MOR agonist DAMGO at 10 μM stimulated the [³⁵S]GTPγS binding by 136 ± 1.7% of the basal activity; DAMGO-induced stimulation was completely antagonized by the MOR antagonist naloxone (5 μM). As shown in Table 2, all tested compounds decreased DAMGO-stimulated [³⁵S]GTPγS binding in a concentration-dependent manner.

Specifically, at the highest concentration tested, almost all compounds decreased DAMGO-induced GTPγS stimulation of 52% and 79%. Indeed, according to data and respective SEM values, the rank order of potency was **9** > **8** = **11** > **10**, respectively. Compounds up to 100 μM (data not shown) did not increase basal [³⁵S] GTPγS binding, thus demonstrating no intrinsic agonist activity.

Compounds **14** and **15**, tested under the same conditions, were almost inactive. In fact, at the highest concentration (10 μM), **14** and **15** inhibited GTPγS stimulation by DAMGO of 15% and 26%, respectively.

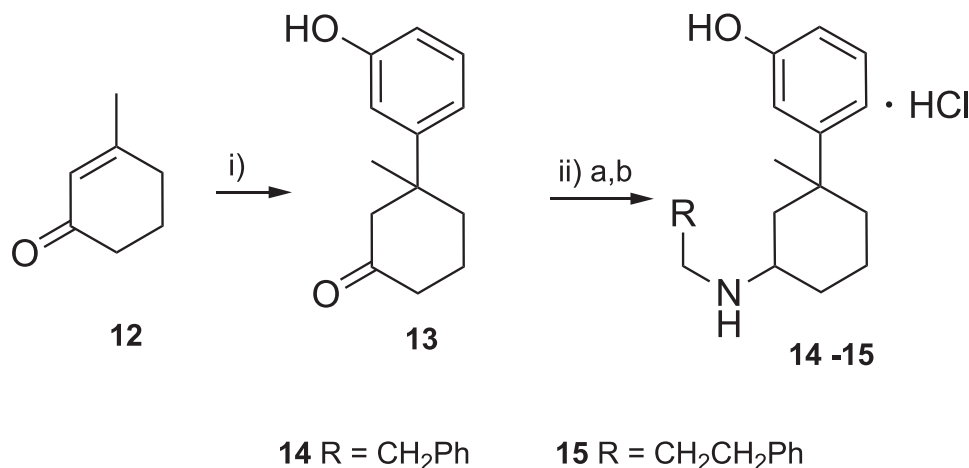
2.3 | In silico study

To provide useful information on the nature of the ligand–receptor interactions, an in silico study was performed on the novel derivatives to identify the most promising stereoisomers. The feasible binding mode was investigated by means of a purpose-built and validated MOR

TABLE 1 Percentage of displacement of SB [³H]DAMGO from rat brain membranes by compounds **8**, **9**, **10**, **11**, **14**, and **15**

Compound	0.01 μM	0.1 μM	1 μM	10 μM
DAMGO	90 ± 2.30	98 ± 0.28	99 ± 0.29	100 ± 0.01
8	4 ± 1.40	33 ± 1.33	83 ± 0.57	98 ± 0.37
9	44 ± 0.88	86 ± 0.58	98 ± 0.33	99 ± 0.88
10	8 ± 0.58	40 ± 0.57	87 ± 0.88	88 ± 0.88
11	7 ± 0.88	23 ± 1.76	75 ± 0.33	99 ± 0.01
14	0	0	5 ± 0.30	15 ± 0.80
15	0	0	4 ± 0.20	17 ± 0.80

Note: Data are mean ± SEM of three to four experiments, each performed in triplicate. DAMGO ([D-Ala², NMe-Phe⁴, Gly-ol⁵]-enkephalin) is our reference compound.



SCHEME 2 Synthesis of compounds **14** and **15**. Reagents and conditions: (i) cat. (CF₃CO₂)₂Pd, (S)-tBuPyOx, ClCH₂CH₂Cl; (ii) a. RCH₂NH₂, NaBH(OAc)₃, MeOH; b. 4 N HCl/Et₂O.

TABLE 2 Effects of compounds **8**, **9**, **10**, **11**, **14**, and **15** on the stimulation of [³⁵S]GTPγS binding via MOR in rat cortical membranes

Compound	μM	Decrease relative to 10 μM of DAMGO %
	Control	0
8	1	31 ± 0.88
	5	48 ± 4.05
	10	57 ± 3.0
9	1	32 ± 2.60
	5	55 ± 7.62
	10	79 ± 6.10
10	1	16 ± 0.33
	5	28 ± 4.05
	10	52 ± 3.80
11	1	31 ± 0.57
	5	43 ± 4.60
	10	59 ± 3.50
14	1	5 ± 0.18
	5	5 ± 0.70
	10	15 ± 0.68
15	1	7 ± 0.18
	5	8 ± 0.80
	10	26 ± 0.70

Note: Data are mean ± SEM of three to four experiments, each performed in triplicate. As the maximal effect of 10 μM DAMGO ([D-Ala², NMe-Phe⁴, Gly-ol⁵]-enkephalin) alone differed between experiments, data were normalized to the effect of 10 μM DAMGO (control, set as 0%). DAMGO at 10 μM stimulated [³⁵S]GTPγS (5'-O-(3-[³⁵S] thiotriphosphate binding to approximately 136 ± 1.7% of the basal activity (set as 100%).

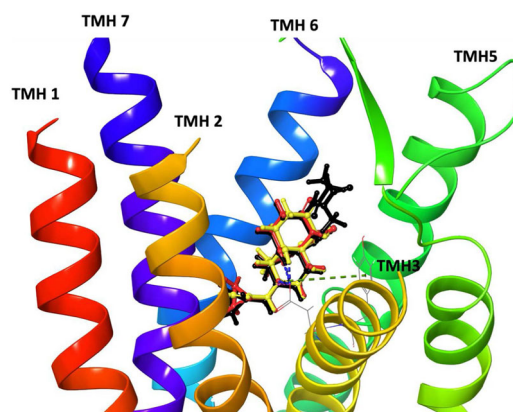
virtual model that was used to carry out a Glide-XP protocol. Thus, the first part of the study was dedicated to the model creation and to the identification of the ligand-receptor interactions. In this regard, the crystal structure of the complex «receptor-BF0 ligand» (PDB 4DKL, Chain A) was used as the framework of choice and the model was then validated by docking and scoring naloxone and naltrexone by means of the Glide-XP algorithm.^[14,15] Each compound was docked as a chiral positively charged amine since at physiological pH the selected drugs are present as protonated forms.^[16] Moreover, to get more reliable results in terms of binding affinities predictions, an MM-GBSA post-processing method was applied.^[17,18] In fact, although molecular docking methods provide excellent binding poses of the ligands within the receptor pocket, they, alone, often fail in predicting suitable binding affinities.^[19–21] Ideally, the MM-GBSA scores should be compared to experimental binding affinities (*K_i*) and measurements taken from human opioid receptors. Docking, ligand-protein binding free energy, and experimental *K_i*^[22] data are reported in Table 3.

TABLE 3 *K_i*, Glide-XP, and MM-GBSA scores of BF0, naltrexone, and naloxone

Compound	Glide-XP (kcal/mol)	MM-GBSA (kcal/mol)	<i>K_i</i> ± SEM (nM) ^{[22] a}
BF0	−9.813	−85.68	–
Naltrexone	−9.171	−76.42	0.23 ± 0.05
Naloxone	−9.067	−71.06	0.79 ± 0.02

Abbreviations: Glide-XP, extra-precision Glide; MM-GBSA, generalized Born surface area; MOR, μ-opioid receptor.

^a*K_i* for the Inhibition of opioid binding measured in CHO cells stably transfected with the human MOR.

**FIGURE 2** Superimposition of the lowest energy poses of BF0 (black), naltrexone (red), and naloxone (yellow) within the MOR pocket. MOR, μ-opioid receptor.

The superimposition of the lowest energy poses of the three antagonists in the MOR binding pocket is depicted in Figure 2. This helped us to identify the common crucial ligand-receptor areas of interaction.

Using the naltrexone molecule as a representative structure, we evidenced the relevant ligand-receptor interactions (Figure 3). In more detail, a strong ionic bond and H-bond between the piperidine's protonated nitrogen and Asp147 on TM3 helix (TMH 3), crucial to locate the ligand inside the receptor, was observed. The same Asp147 residue was also involved in an electrostatic contact with the alcoholic group, while Tyr 148 (TMH 3), engaged a π-cation interaction with piperidine's protonated nitrogen. Interestingly, we observed a water bridge formation involving the phenolic hydroxyl moiety and the Lys 233 residue on the TM5 helix (TMH 5). Moreover, due to its high lipophilic nature, naltrexone showed many hydrophobic interactions. A π-π stacking occurred between the phenyl ring and Hys 297 on the TM6 helix (TMH 6), while the cyclopropyl chain, directed toward the inner part of the receptor, interacted mainly with Trp 293 (TMH 6), Ile 322 and Tyr 326 (TMH 7). Instead, the morphinan scaffold is oriented towards the outer part of the pocket where engaged van der Waals contacts particularly with Met151 (TMH 3), Val 236 (TMH 5), Ile 296, Hys 297, and Val 300 on TMH 6, and Trp 318 on TMH 7.

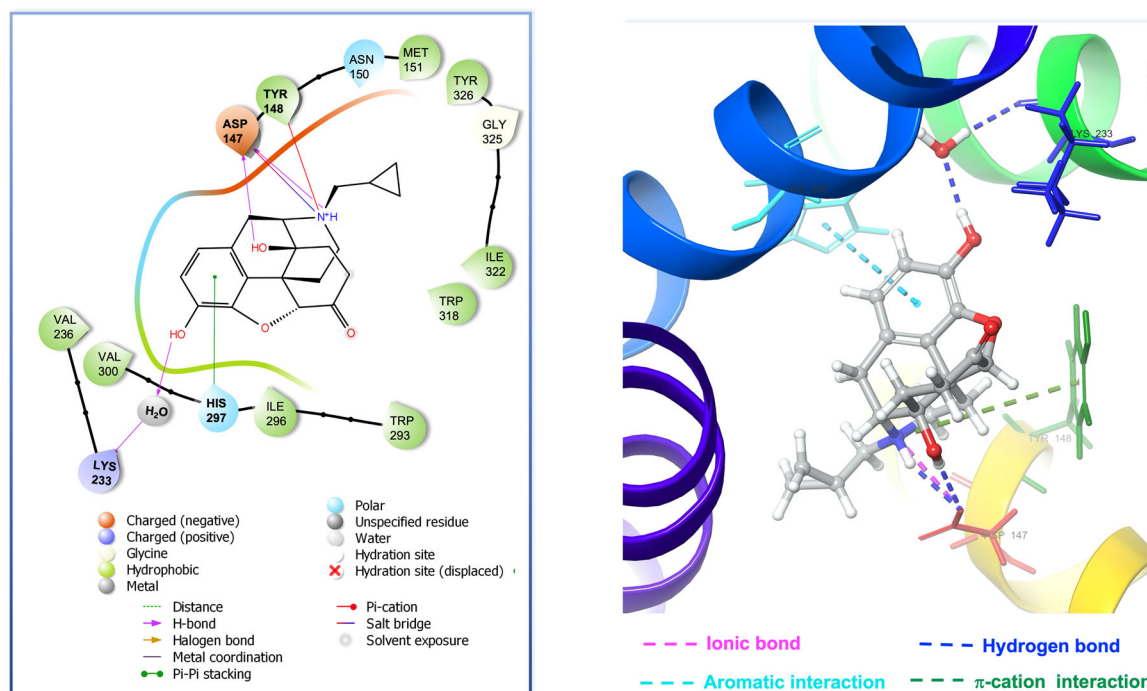


FIGURE 3 Binding site molecular models of MOR/naltrexone complex obtained with Glide-XP. Glide-XP, extra-precision Glide; MOR, μ -opioid receptor.

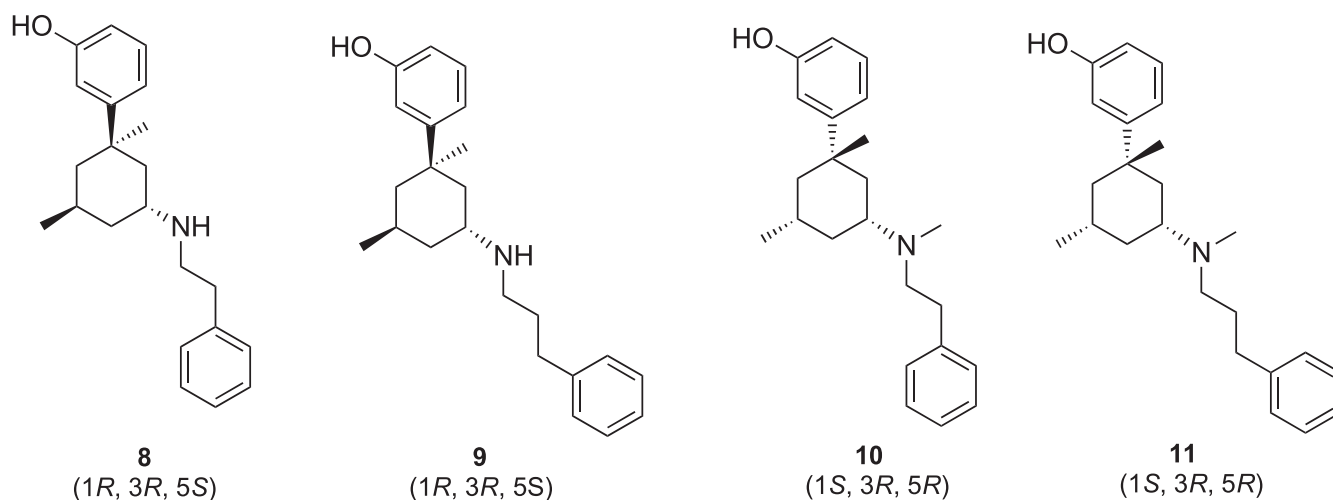


FIGURE 4 Best stereoisomers coming from virtual screening approach

In the second part of the in-silico study, the previously created virtual MOR model was then used to investigate all the stereoisomers belonging to the newly synthesized 3-[3-(phenalkylamino)cyclohexyl]phenols, applying the Glide-XP algorithm to carry out the docking experiments. The best 25 docking poses of each ligand have been elected to be considered for further MM-GBSA investigation. A molecular mechanic method (embedded in the Prime module of Schrodinger Suite) based on MM-GBSA with default parameters and implicit membrane and solvent, was used to calculate the free-binding energy of all complexes. The most promising stereoisomers with the lowest MM-GBSA score are shown in Figure 4 and Table 4.

Afterward, we identified and investigated the ligand-MOR interactions for every compound reported above. The observation of the two- and three-dimensional representation of the MOR binding pocket, enabled the putative binding modes and the molecular interactions to be determined. Importantly, all the compounds displayed a strong ionic contact with Asp147 that stabilized the ligand inside the receptor but, differences in terms of N-phenylalkyl chain length and in nitrogen substitution could plausibly be related to their peculiar orientation within the binding pocket. Table 4 shows that compound (1R, 3R, 5S) **9**, with the lowest MM-GBSA score, exhibited the best MOR-ligand complex stability.

Interestingly, its equatorially oriented phenol moiety, as already observed for naltrexone, showed the OH group involved in a water bridge interaction with Lys 233. Moreover, the same hydroxyl group displayed an H bond contact with the Tyr 148 residue while stabilization of the phenyl propyl chain inside the binding pocket was due to a π - π stacking with Tyr 128 on TMH 2 (Figure 5).

Noteworthy, compound (1R, 3R, 5S) **8**, showed Glide and MM-GBSA scores higher than (1R, 3R, 5S) **9**, indicating that the replacement of the phenyl propyl chain with a phenyl ethyl one could affect both the binding affinity and MOR-ligand complex stability. Although the absolute stereochemistry and the phenol moiety equatorial orientation remained unchanged, compound **8**, with

TABLE 4 Docking and free binding energy scores for the best stereoisomers of compounds **8**, **9**, **10**, and **11**

Compound	Glide-XP (kcal/mol)	MM-GBSA (kcal/mol)
(1R, 3R, 5S) 9	-7.727	-70.41
(1S, 3R, 5R) 10	-6.044	-69.15
(1R, 3R, 5S) 8	-7.393	-68.68
(1S, 3R, 5R) 11	-8.261	-68.27

Abbreviations: Glide-XP, extra-precision Glide; MM-GBSA, generalized Born surface area; MOR, μ -opioid receptor.

respect to **9**, appeared differently placed inside the pocket. Possibly consistent with the different carbon chain lengths, the phenyl ethyl moiety of **8** was oriented towards the TMH 5, engaging a π -cation interaction with Lys 233. Instead, the phenol group pointed toward TMH 3 with OH engaging H bonds with both Asp 147 and Asn 150 (Figure 6).

N-Methyl substitution on **8** generated derivative **10**, whose (1S, 3R, 5R) stereoisomer showed 1,3-*cis* orientation and a lower MM-GBSA value. This increased stability might be related to a different orientation of the molecule that provided compound **10**, with respect to **8**, a larger number of interactions with the binding pocket (Figure 7). In particular, the protonated nitrogen atom engaged an ionic bond and an H-bond with Asp147, which is also involved in a π -cation contact with Tyr 148. Moreover, the phenol moiety, oriented toward TMH 7, formed H bonds with Trp 318 and His 319 while the phenyl ethyl group engaged a π - π stacking with Trp 293.

Conversely, replacement of NH with N-CH₃, appeared detrimental for **9** as the emerging derivative (1S, 3R, 5R) **11** showed the worst free binding energy score (Table 4). As already observed for **10**, the steric effect of the N-methyl group might be suggestive of the stereochemistry inversion at C-1 and C-5 and the 1,3-*cis* orientation. Interestingly, compounds **9** and **11** best poses, although similarly placed within MOR, differed mainly in the orientation of either the

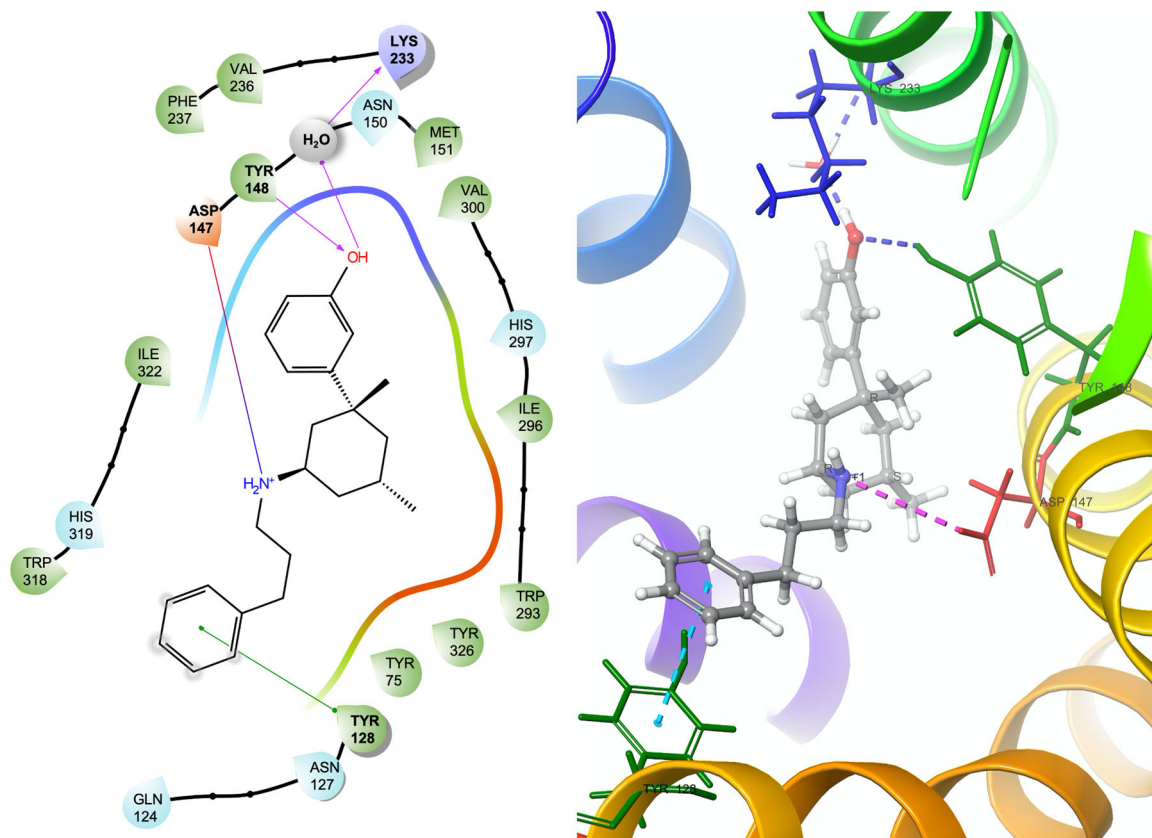


FIGURE 5 Binding site molecular models of MOR/**9** complex obtained with Glide-XP. Glide-XP, extra-precision Glide; MOR, μ -opioid receptor.

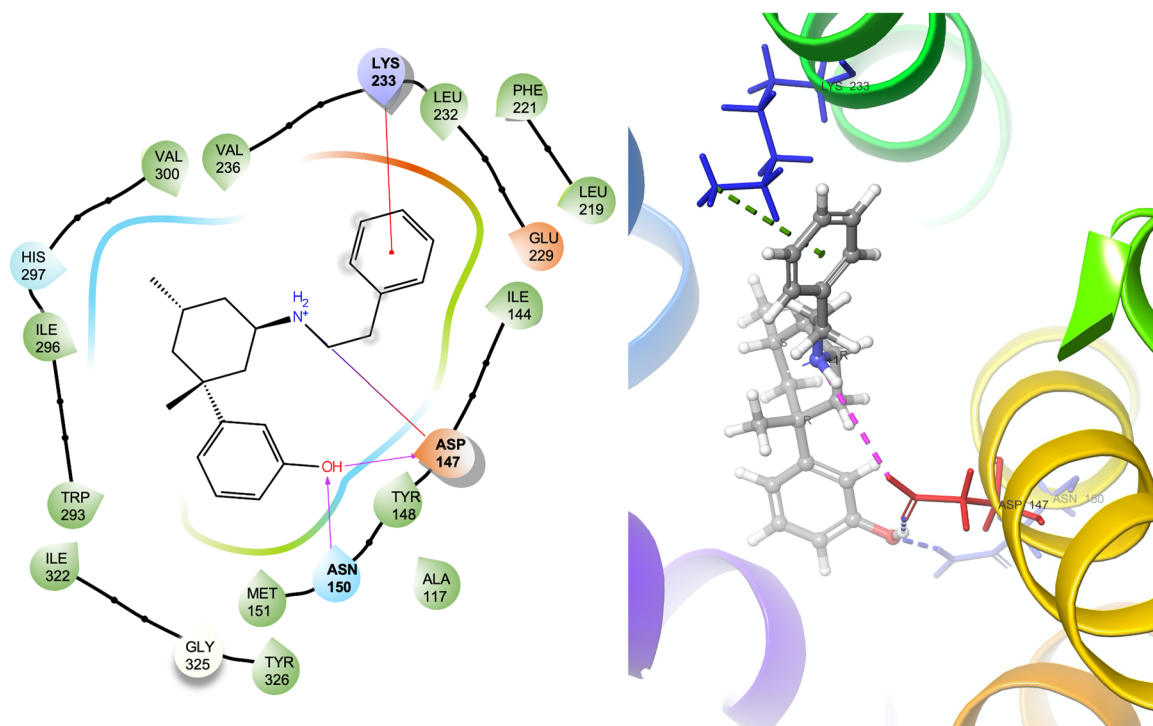


FIGURE 6 Binding site molecular models of MOR/8 complex obtained with Glide-XP. Glide-XP, extra-precision Glide; MOR, μ -opioid receptor.

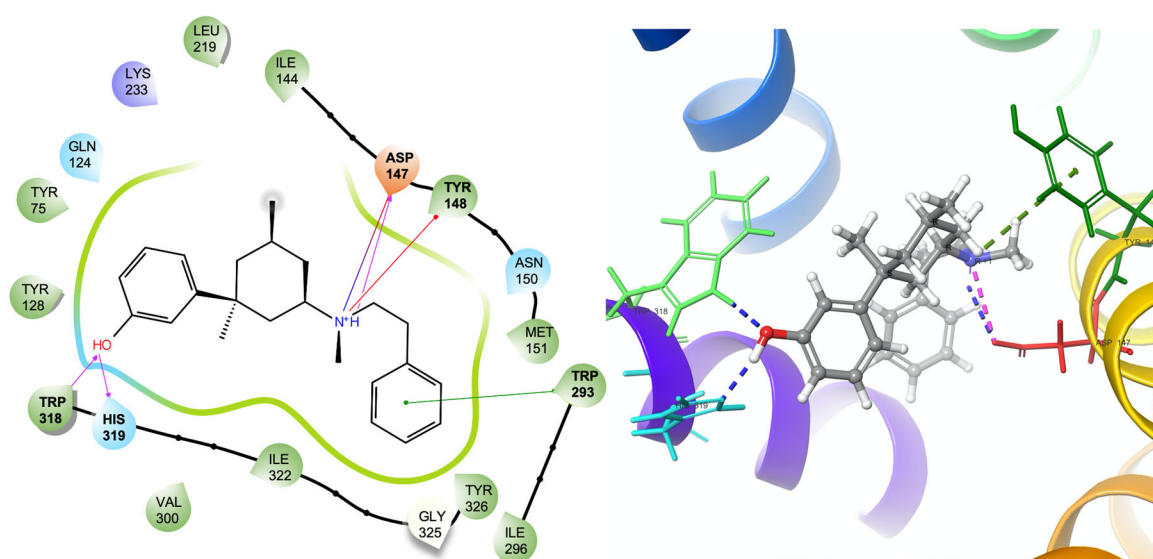


FIGURE 7 Binding site molecular models of MOR/10 complex obtained with Glide-XP. Glide-XP, extra-precision Glide; MOR, μ -opioid receptor.

phenyl alkyl and the phenol substituents that are now directed toward TMH 2 and TMH 6, respectively (Figure 8).

Moreover, Figure 9 shows that compound 11, apart from the ionic and hydrogen bond with Asp 147, displayed only a water bridge between OH phenolic group and His 297.

Besides, to better explore the receptor conformational features involved in the deactivation mechanism, Glide-XP and MM-GBSA

experiments were also carried out with the most promising (1R, 3R, 5S) 9 on the active form of MOR bound to the crystal morphinan agonist BU72.

Even here, we observed that the strong ionic contact with Asp 147 was crucial to locating the ligand inside the receptor as well as the hydrophobic interactions with receptor sub-pocket residues. However, when located in MOR active form, compound (1R, 3R, 5S) 9

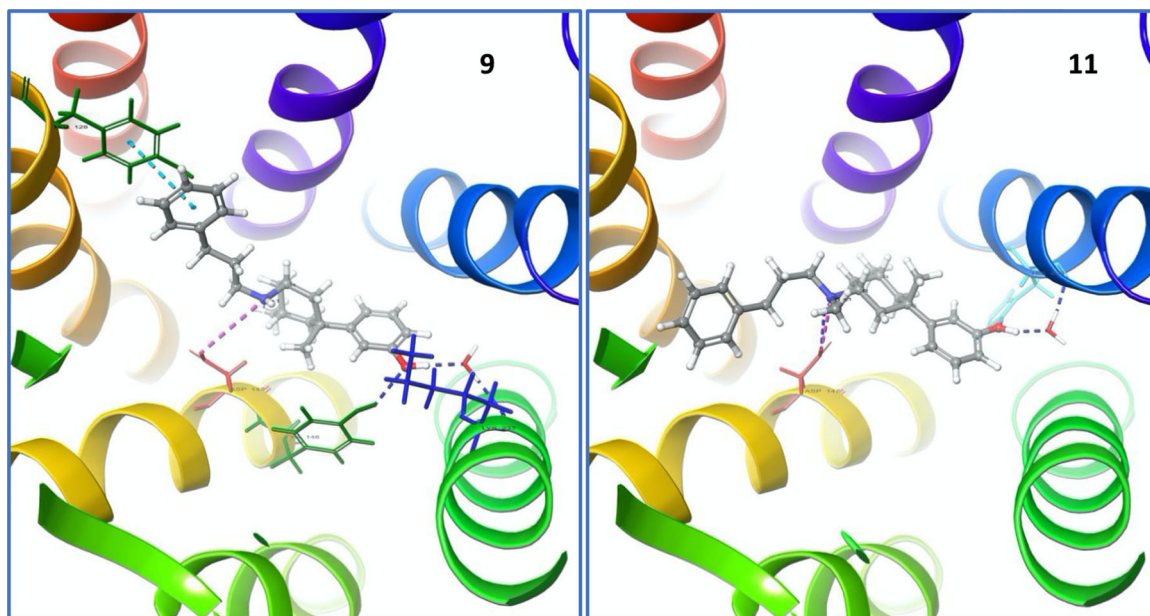


FIGURE 8 Comparison between **9** and **11** within MOR binding site. MOR, μ -opioid receptor.

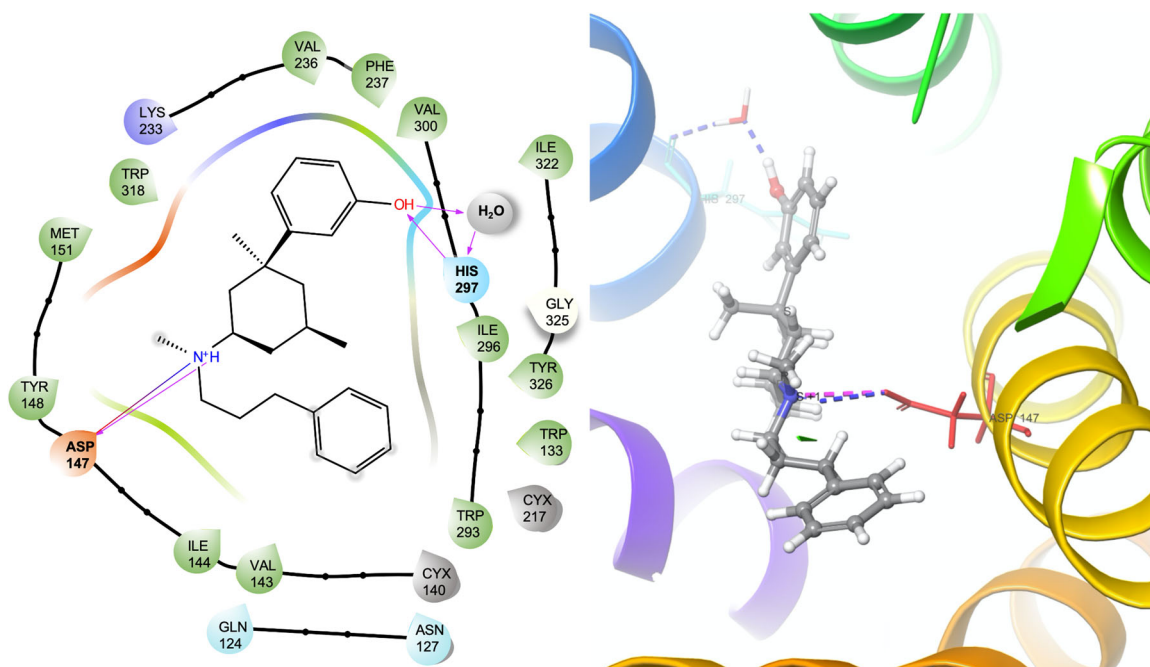


FIGURE 9 Binding site molecular models of MOR/**11** complex obtained with Glide-XP. Glide-XP, extra-precision Glide; MOR, μ -opioid receptor.

showed a novel π - π interaction between the phenol moiety and Tyr 148, not displaying the water bridge between OH group and Lys 233 anymore (Figures 10 and 11).

Thus, preliminary investigations carried out on our first 3-[3-(phenalkylamino)cyclohexyl]phenol derivatives, indicated the importance of a peculiar combination of C-1 stereochemistry and *N*-substitution. In particular, ligands **8** and **9** supporting a secondary amino group, suggested the importance of the carbon chain length effect

for a favorable orientation of the molecule inside MOR. On the contrary, the presence of a methyl group on aminic nitrogen appeared determinant for ligand stereochemistry, that is, the most promising stereoisomers of **10** and **11** showed an inverted stereochemistry at C-1 and C-5, still supporting a 1,3-*cis eq* orientation. Noteworthy, a comparison between **9** and **11**, highlighted that, although exhibiting a similar pose inside the receptor, the different stereochemistry at C-1 and C-5, made **11** the compound with the lowest MM-GBSA score. The low stability of

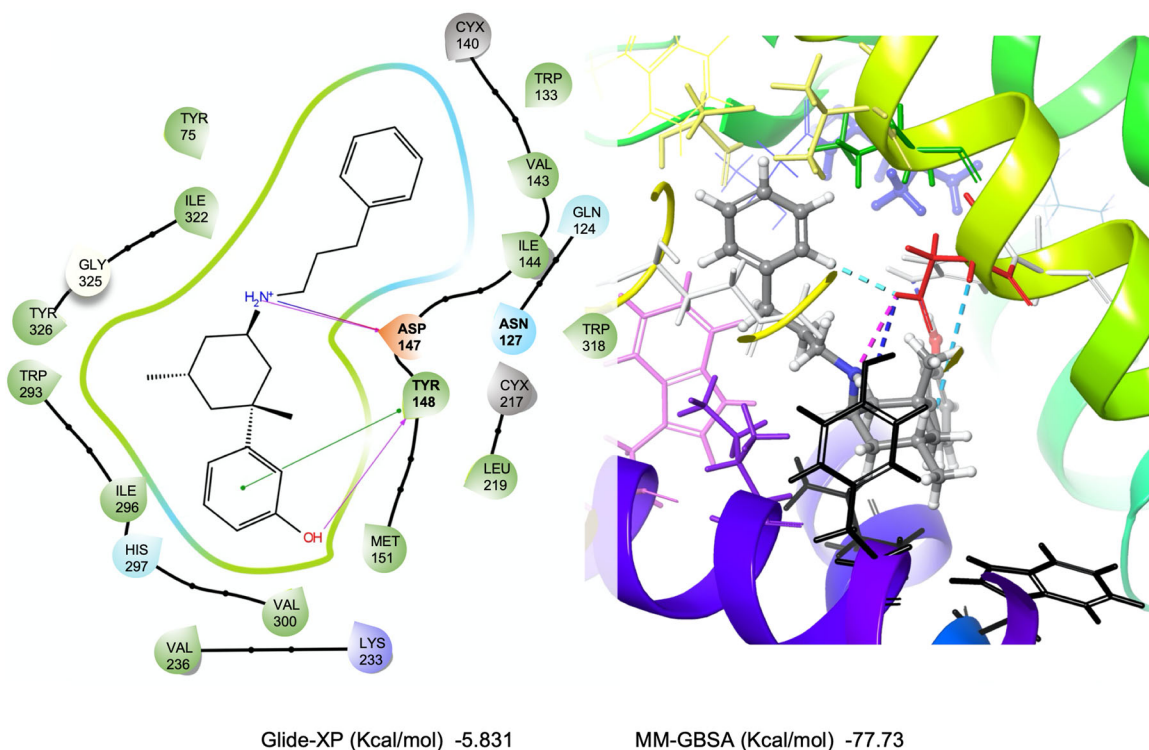


FIGURE 10 Binding site molecular models of MOR active form/9 complex obtained with Glide-XP. Glide-XP, extra-precision Glide; MOR, μ -opioid receptor.

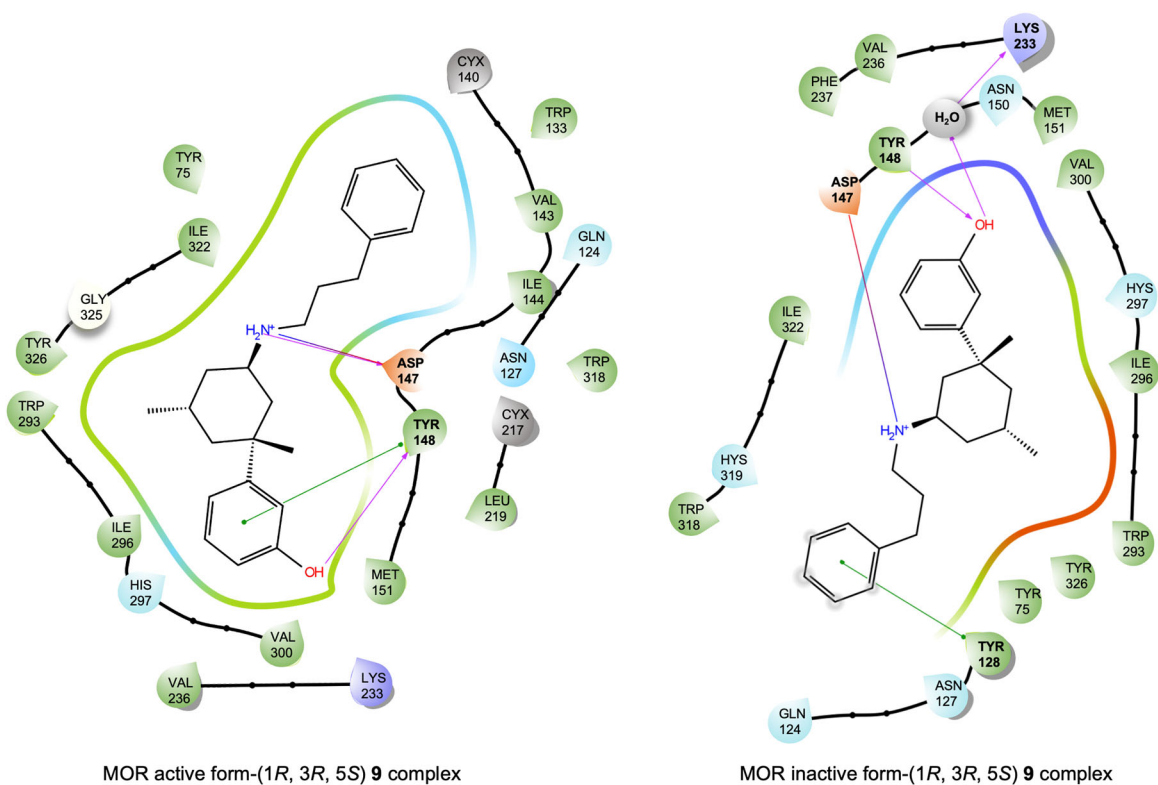


FIGURE 11 MOR-(1R, 3R, 5S) 9 complex: MOR active form versus MOR inactive form. MOR, μ -opioid receptor.

the 11-receptor complex might be a consequence of the loss of the water bridge interaction with Lys 233, the hydrogen bond contact with the Tyr 148, and the π - π stacking between the phenyl propyl chain with Tyr 128.

Interestingly, the methyl group (R) in position 5 to cyclohexane ring might be important not only as a conformation stabilizer but also as a potential modulator of biological activity, as suggested by compounds **14** and **15**.

Moreover, the loss of the water bridge interaction between the phenolic OH and Lys 233 when (1R, 3R, 5S) **9** is bound to MOR-active form might suggest its possible role in receptor deactivation as it is also present in MOR inactive form-naltrexone complex.

3 | CONCLUSION

In conclusion, using naltrexone as a structural prototype and applying a simple synthetic approach, we disclosed the first examples of novel 3-[3-(phenalkylamino)cyclohexyl] phenol analogs that were designed, synthesized, and evaluated in vitro and in silico.

Racemic compounds were tested for their ability to displace [^3H] DAMGO from its binding site in a membrane preparation of rat brain (minus cerebellum). Moreover, almost all derivatives, at the highest concentrations tested decreased DAMGO-induced GTPyS stimulation between 52% and 75%, suggesting that they acted as antagonists, counteracting the activation of a G-protein coupled MOR. Then, the ligand structural requirements were investigated by an in silico MOR model ad hoc developed. Docking and MM-GBSA experiments provided useful information on the nature of ligand-receptor interactions and stability. Structural differences in terms of stereochemistry, *N*-substitution, and chain length of the phenalkylamino group led us to speculate about the molecular basis of their different MOR binding affinity.

The comparison between compounds **8** and **9** underlined that the longer phenyl propyl chain, although not affecting the absolute stereochemistry and the equatorial orientation of the phenol ring, differently placed **9** within the binding pocket, allowing the ligand to engage a larger number of interactions, particularly an additional π - π stacking between the phenylpropyl chain with Tyr 128. Specifically, the added interaction with TMH 2 might be liable for the higher stability of the (1R, 3R, 5S) **9**-receptor complex. The replacement of the NH group with an *N*-CH₃ generated compound **11**, whose best stereoisomer exhibited a different stereochemistry at C-1 and C-5 that might be liable for its worst free binding energy score. In fact, the different orientations of both the phenylpropyl and the phenol moieties were likely responsible for the loss of many of the interactions that, conversely, stabilized compound **9** within MOR.

A different situation was observed in the presence of the shorter phenyl ethyl alkyl chain. In this case, the stereochemistry inversion induced by the *N*-CH₃ substitution positively affected the protein-ligand complex stability. In fact, (1S, 3R, 5R) **10** gained additional contacts than the ligand (1R, 3R, 5S) **8**, particularly with Tyr 148, Trp 293, Trp 318, and His 319.

Interestingly, compound **9** showed the best binding affinity, the highest ability to decrease DAMGO-induced GTPyS stimulation, and the finest MOR-ligand complex stability. Further experiments will be then focused on designing stereoselective procedures for the synthesis of the best emerging 3-[3-(phenalkylamino)cyclohexyl]phenol stereoisomers.

4 | EXPERIMENTAL

4.1 | Chemistry

4.1.1 | General

Unless otherwise stated, all materials were obtained from commercial suppliers and used without further purification. All reactions were performed under an argon atmosphere unless otherwise indicated. All final compounds are >95% pure by high-performance liquid chromatography (HPLC) analysis. Reagents and starting materials were obtained from commercial sources and used as received. The solvents were purified and dried by standard procedures before use; petroleum ether of boiling range 60–80°C was used. Flash chromatography was carried out using Merck Kieselgel (230–400 mesh). NMR spectra were recorded on Varian Mercury (400 MHz) and Bruker (300 MHz) spectrometers. Chemical shift values are referenced against residual protons in the deuterated solvents, multiplicity (s = singlet, d = doublet, t = triplet, q = quartet, m = multiplet, br = broad). *J* values are reported in Hertz. Liquid chromatography-mass spectrometry (LC-MS) analyses were performed on Shimadzu CBM–20 A with Applied Biosystems API 2000 mass detector. HRMS were obtained on a Waters Synapt G2-Si mass spectrometer coupled with Acquity UPLC H-Class Column. Thin-layer chromatography performed on DC Alufolien, Kieselgel 60 F₂₅₄ (Merck) plates; UV detection. Flash column chromatography was carried out using silica gel (Merck silica gel 60). The purity of all compounds was determined by HPLC on a Shimadzu CBM–20 A (HPLC column: Phenomenex Gemini C18, 50 × 2 mm, 5 μm). Method I—gradient: from 10% MeCN/0.1% HCO₂H to 90% MeCN/0.1% HCO₂H in 12 min, hold 3 min 90% MeCN/0.1% HCO₂H.

4.1.2 | Synthesis of 3-(3-methoxyphenyl)-5-methylcyclohex-2-en-1-one (**2**)

To magnesium turnings (2.61 g, 99 mmol) in dry Et₂O (7 ml) few crystals of iodine were added, followed by a dropwise addition of 3-bromoanisole (16.83 g, 90 mmol) solution in dry Et₂O. The reaction mixture was stirred at reflux for 50 min and cooled down. Then, a solution of 3-ethoxy-5-methylcyclohex-2-en-1-one **1** (7.33 g, 47.56 mmol) in Et₂O (25 ml) was added dropwise. After the addition was complete the reaction mixture was stirred at reflux for 30 min, cooled with ice water, and treated with

50 mL of 1 N aqueous HCl. Then brine was added, the mixture extracted with Et₂O and the combined organic extracts dried over Na₂SO₄. The solution was filtered and concentrated. The crude product was purified by flash chromatography on silica gel eluting with hexane/EtOAc mixture to give the title compound **2** (8.40 g, 82%) as a yellow oil. ¹H NMR (400 MHz, CDCl₃) δ: 7.32 (t, *J* = 8.0 Hz, 1H), 7.12 (ddd, *J* = 7.8, 1.7, 0.9 Hz, 1H), 7.05 (dd, *J* = 2.5, 1.7 Hz, 1H), 6.95 (ddd, *J* = 8.2, 2.5, 0.9 Hz, 1H), 6.40 (d, *J* = 2.3 Hz, 1H), 3.83 (s, 3H), 2.82 (dd, *J* = 17.0, 3.8 Hz, 1H), 2.60–2.50 (m, 1H), 2.48–2.38 (m, 1H), 2.39–2.26 (m, 1H), 2.17 (dd, *J* = 16.2, 11.8 Hz, 1H), and 1.16 (d, *J* = 6.4 Hz, 3H) ppm.

4.1.3 | 3-(3-Methoxyphenyl)-3, *cis*-5-dimethylcyclohexan-1-one (**3**)

To the suspension of CuCl (80.7 mg, 815 μmol) in anhydrous Et₂O (8 ml) cooled to –20°C under argon atmosphere was added dropwise 3 M methyl magnesium chloride in THF (3.00 ml, 9 mmol). After 1 h the reaction mixture was warmed to –10°C and a solution of **2** (1.3 g, 6.0 mmol) in dry THF (7 ml) was added dropwise within 30 min. The mixture was slowly warmed to room temperature and stirred for 1 h. The reaction was quenched by the addition of saturated aqueous ammonium chloride. The layers were separated and the aqueous layer was extracted with EtOAc. The organic phase was washed with brine, dried over anhydrous Na₂SO₄, filtered, and concentrated in vacuo. The residue was purified by flash chromatography eluting with hexane/EtOAc mixture to give compound **3** (615 mg, 44%) as a white solid. ¹H NMR (400 MHz, CDCl₃) δ: 7.28 (t, *J* = 8.0 Hz, 1H), 6.95 (ddd, *J* = 7.9, 1.9, 0.9 Hz, 1H), 6.90 (t, *J* = 2.2 Hz, 1H), 6.77 (ddd, *J* = 8.2, 2.2, 0.9 Hz, 1H), 3.82 (s, 3H), 2.64 (d, *J* = 13.2 Hz, 1H), 2.50 (dt, *J* = 13.1, 2.3 Hz, 1H), 2.44 (ddt, *J* = 13.5, 4.2, 2.0 Hz, 1H), 2.25–2.11 (m, 1H), 2.06–1.97 (m, 2H), 1.74–1.64 (m, 1H), 1.26 (s, 3H), and 1.09 (d, *J* = 6.3 Hz, 3H) ppm.

4.1.4 | General procedure for the synthesis of *N*-phenethyl 3-(3-methoxyphenyl)-3,5-dimethylcyclohexan-1-amine (**4**) and of *N*-phenylpropyl 3-(3-methoxyphenyl)-3,5-dimethylcyclohexan-1-amine (**5**)

To the solution of **3** (200 mg, 861 μmol) in MeOH (4 ml) the corresponding primary amine (1.33 mmol, 1.2 equiv) was added and the resulting mixture was stirred for 5 min, then NaBH₃CN (108 mg, 1.72 mmol, 2 equiv) was added. The reaction mixture was stirred at room temperature for 16 h, then it was concentrated under reduced pressure. The mixture was treated with water and then extracted with EtOAc. The organic extracts were dried over Na₂SO₄, evaporated, and used in the next step without further purification.

4.1.5 | General procedure for the synthesis of benzyl [3-(3-methoxyphenyl)-3,5-dimethylcyclohexyl](phenethyl)carbamate (**6**) and of benzyl [3-(3-methoxyphenyl)-3,5-dimethylcyclohexyl](phenylpropyl)carbamate (**7**)

To the solution of corresponding amine **4** or **5** from the previous step (1 equiv) and Et₃N (2 equiv) in acetonitrile at ice bath temperature was added dropwise a solution of CbzCl (1.1 equiv) in dry MeCN. The reaction mixture was stirred at room temperature for 20 h (reaction control by LC/MS). Then water was added, the mixture was extracted with EtOAc, and the organic phase, previously dried over Na₂SO₄, was evaporated. The crude mixture was purified on silica gel eluting with EtOAc/petroleum ether (1:10).

Benzyl [3-(3-methoxyphenyl)-3,5-dimethylcyclohexyl](phenethyl)carbamate (**6**) was obtained with a 73% yield, starting from compound **3** and phenethylamine. ¹H NMR (400 MHz, CDCl₃) δ: 7.45–7.31 (m, 5H), 7.30–7.15 (s, 5H), 7.15–6.88 (m, 3H), 6.75–6.65 (m, 1H), 5.28–5.19 (m, 2H), 4.46 (t, *J* = 12.6 Hz, 1H), 3.89–3.71 (m, 3H), 3.50–3.28 (m, 2H), 3.04–3.73 (m, 2H), 2.42–2.08 (m, 2H), 1.84–1.66 (m, 1H), 1.60–1.41 (m, 1H), 1.41–1.19 (m, 1H), 1.19–1.07 (m, 3H), 0.98–0.83 (m, 2H), and 0.50 (br d, *J* = 7.6 Hz, 3H) ppm. LC/MS: *m/z* 471.8 [M]⁺.

Benzyl [3-(3-methoxyphenyl)-3,5-dimethylcyclohexyl](phenylpropyl)carbamate (**7**) was obtained with 52% yield, starting from compound **3** and 3-phenylpropylamine. ¹H NMR (400 MHz, CDCl₃) δ: 7.46–6.83 (m, 13H), 6.79–6.57 (m, 1H), 5.26–5.12 (m, 2H), 4.38 (tt, *J* = 12.5, 3.7 Hz, 1H), 3.90–3.68 (m, 3H), 3.34–3.10 (m, 2H), 2.71–2.52 (m, 2H), 2.35 (d, *J* = 11.2 Hz, 1H), 2.20 (d, *J* = 13.2 Hz, 1H), 2.15–2.06 (s, 1H), 2.01–1.82 (m, 2H), 1.78–1.61 (m, 1H), 1.62–1.42 (m, 4H), 1.14 (s, 3H), 0.98–0.87 (m, 2H), and 0.49 (d, *J* = 7.2 Hz, 3H) ppm. LC/MS: *m/z* 485.6 [M]⁺.

4.1.6 | General procedure for the synthesis of 3-[1,5-dimethyl-3-(phenethylamino)cyclohexyl]phenol hydrochloride (**8**) and of 3-[1,5-dimethyl-3-(3-phenylpropylamino)cyclohexyl]phenol hydrochloride (**9**)

Carbamates **6** or **7** (1 equiv.) were dissolved in CH₂Cl₂ (1 mmol/4.5 ml) and cooled on a dry ice-acetone bath at –78°C, while 0.1 M BBr₃ in CH₂Cl₂ (2.5 equiv) was added dropwise over 30 min. The resulting chalky solution was allowed to warm to room temperature and stirred for 15 h under an argon atmosphere. The mixture was hydrolyzed by shaking with H₂O (5 ml/mmol), neutralized with aqueous NaHCO₃, and extracted with CH₂Cl₂. The organic extract was dried over Na₂SO₄ and evaporated under reduced pressure. The crude product was purified by flash chromatography on reversed-phase column, then by preparative HPLC. Product-containing fractions were concentrated by evaporation, treated with 4 N HCl in diethyl ether and the precipitate was dried in vacuo.

3-[1,5-Dimethyl-3-(phenethylamino)cyclohexyl]phenol hydrochloride (**8**) was obtained as a white solid with a 36% yield. ^1H NMR: (400 MHz, CDCl_3) δ : 9.16 (br. s, 1H), 9.00 (br. s, 1H), 7.30–7.19 (m, 3H), 7.18–7.11 (m, 3H), 7.01 (t, $J = 2.1$ Hz, 1H), 6.82 (d, $J = 8.0$ Hz, 1H), 6.69 (dd, $J = 8.1, 2.4$ Hz, 1H), 4.85 (br. s, 1H), 3.62 (m, 1H), 3.32–3.10 (m, 2H), 3.10–2.97 (m, 2H), 2.63 (d, $J = 13.0$ Hz, 1H), 2.24–2.12 (m, 2H), 1.81–1.65 (m, 1H), 1.65–1.55 (m, 1H), 1.53 (t, $J = 12.6$ Hz, 1H), 1.04 (s, 3H), and 0.44 (d, $J = 7.3$ Hz, 3H) ppm. ^{13}C NMR: (100 MHz, CDCl_3) δ : 156.84, 148.50, 136.07, 129.91, 129.11, 128.77, 127.48, 118.18, 112.91, 111.80, 51.42, 45.49, 42.45, 39.56, 38.59, 35.86, 33.99, 32.80, 28.01, and 20.14 ppm. HR-MS(ESI): m/z found 324.2321; calcd. 324.2327 for $\text{C}_{22}\text{H}_{30}\text{NO}$ ($[\text{M}+\text{H}]^+$).

3-[1,5-Dimethyl-3-(3-phenylpropylamino)cyclohexyl]phenol hydrochloride (**9**) was obtained as a white solid with a 31% yield. ^1H NMR: (400 MHz, CDCl_3) δ : 9.03 (br. s, 1H), 8.75 (br. s, 1H), 7.79 (br. s, 1H), 7.25–7.07 (m, 7H), 6.83 (d, $J = 7.8$ Hz, 1H), 6.72 (dd, $J = 7.9, 1.9$ Hz, 1H), 3.58–3.47 (m, 1H), 3.07 (br. s, 1H), 2.95 (br. s, 1H), 2.71 (d, $J = 12.6$ Hz, 1H), 2.64 (t, $J = 7.2$ Hz, 2H), 2.25–2.06 (m, 4H), 1.82–1.52 (m, 4H), 1.01 (s, 3H), and 0.44 (d, $J = 7.0$ Hz, 3H) ppm. ^{13}C NMR: (100 MHz, CDCl_3) δ : 156.50, 148.61, 139.81, 129.74, 128.77, 128.43, 126.54, 118.29, 112.87, 112.43, 51.74, 43.88, 42.26, 39.32, 38.64, 35.80, 34.22, 32.79, 27.94, 27.84, and 20.20 ppm. HR-MS(ESI): m/z found 338.2493; calcd. 338.2484 for $\text{C}_{23}\text{H}_{32}\text{NO}$ ($[\text{M}+\text{H}]^+$).

4.1.7 | General procedure for the synthesis of 3-{1,5-dimethyl-3-[methyl(phenylethyl)amino]cyclohexyl}phenol hydrochloride (**10**) and of 3-{1,5-dimethyl-3-[methyl(3-phenylpropyl)amino]cyclohexyl}phenol hydrochloride (**11**)

To the solution of amines **8** or **9** (1 equiv) as free bases in MeOH (1 ml per 0.1 mmol) was added 37% aqueous formaldehyde (2 equiv) and stirred for 30 min, then NaBH_3CN (3 equiv) was added. The reaction mixture was stirred at room temperature for 16 h, then it was concentrated under reduced pressure. To the residue was added aqueous NaHCO_3 , the mixture was extracted with EtOAc and the organic extract was dried over Na_2SO_4 . After solvent evaporation, the crude was dissolved in 4 N HCl and purified by flash chromatography on the reversed-phase column to give compounds **10** or **11** as hydrochloride salts.

3-[1,5-Dimethyl-3-[methyl(phenylethyl)amino]cyclohexyl]phenol hydrochloride (**10**) was obtained as a white solid with 37% yield. ^1H NMR: (400 MHz, CDCl_3) δ : 11.53–11.47 (m, 1H), 7.37–7.16 (m, 7H), 6.87–6.83 (m, 1H), 6.79–6.74 (m, 1H), 3.79–3.75 (m, 1H), 3.65–3.59 (m, 1H), 3.55–3.02 (m, 5H), 2.91 and 2.83 (both s, total 3H), 2.28–2.23 (m, 2H), 1.80–1.76 (m, 2H), 1.58–1.46 (m, 2H), 1.14 (s, 3H), and 0.48 (d, $J = 7.1$ Hz, 3H) ppm. ^{13}C NMR: (100 MHz, CDCl_3) δ : 157.29, 147.69, 136.10, 129.68, 129.05, 128.99, 128.82, 127.30, 117.78, 117.72, 112.99, 112.40, 59.15, 57.20, 55.70, 42.38, 39.35, 36.13, 34.94, 30.91, 30.32, 28.15, and 20.06 ppm. HR-MS(ESI): m/z found 338.2498; calcd. 338.2484 for $\text{C}_{23}\text{H}_{32}\text{NO}$ ($[\text{M}+\text{H}]^+$).

3-[1,5-Dimethyl-3-[methyl(3-phenylpropyl)amino]cyclohexyl]phenol hydrochloride (**11**) was obtained as a white solid with 70% yield. ^1H NMR: (400 MHz, CDCl_3) δ : 11.17 and 10.97 (both br. s, total 1H), 8.22 and 8.11 (both br. s, total 1H), 7.31–7.07 (m, 7H), 6.88–6.79 (m, 1H), 6.75 (dd, $J = 7.9, 2.2$ Hz, 1H), 3.73–3.48 (m, 1H), 3.34–3.21 and 3.05–2.60 (m, 8H), 2.44–1.97 (m, 4H), 1.78–1.39 (m, 4H), 1.13 (s, 3H), 0.52 and 0.48 (both d, $J = 7.3$ Hz, total 3H) ppm. ^{13}C NMR: (100 MHz, CDCl_3) δ : 157.27, 147.80, 139.45, 129.67, 128.74, 128.42, 128.30, 126.59, 126.57, 117.81, 113.00, 112.24, 56.72, 53.82, 42.29, 39.34, 39.13, 38.06, 37.94, 36.16, 35.03, 32.69, 30.29, 28.12, 25.61, and 20.13. HR-MS(ESI): m/z found 352.2645; calcd. 352.2640 for $\text{C}_{24}\text{H}_{34}\text{NO}$ ($[\text{M}+\text{H}]^+$).

4.1.8 | Synthesis of 3-(3-hydroxyphenyl)-3-methylcyclohexan-1-one (**13**)

A screw-top 50 ml vial was charged with a stir bar, $\text{Pd}(\text{CF}_3\text{CO}_2)_2$ (178 mg, 0.537 mmol), (S)-4-(tert-butyl)-2-(pyridine-2-yl)-4,5-dihydrooxazole (131 mg, 0.645 mmol), 3-hydroxybenzeneboronic acid (1 equiv, 740 mg, 5.33 mmol), 2-methylcyclohex-2-en-1-one **12** (1 equiv, 592 mg, 5.37 mmol) and 1,2-dichloroethane (10 ml). The vial was sealed with a PTFE/silicone-lined septum cap and the reaction mixture was stirred at 80°C for 3 h. Then another equivalent of 3-hydroxybenzeneboronic acid (1 equiv, 740 mg, 5.33 mmol) was added and the reaction mixture was stirred for another 3 h. The same procedure was followed for the third equivalent of 3-hydroxybenzeneboronic acid (1 equiv, 740 mg, 5.33 mmol). The reaction mixture was filtered through a short plug of silica gel, eluting with EtOAc. The solvent was evaporated, and the crude was purified on silica gel, eluting with hexane/EtOAc (10:1) ($R_f = 0.18$, EtOAc/hexane, 1:8). This procedure gave the desired compound **13** as a colorless oil (650 mg, 59%). ^1H NMR: (300 MHz, CDCl_3) δ : 7.23 (t, $J = 7.8$ Hz, 1H), 7.09–7.06 (m, 2H), 6.72–6.68 (m, 1H), 2.84 (d, $J = 15$ Hz, 1H), 2.38 (d, $J = 15$ Hz, 1H), 2.30–2.26 (m, 2H), 2.16–2.10 (m, 1H), 1.87–1.76 (m, 2H), 1.66–1.53 (m, 1H), and 1.25 (s, 3H) ppm.

4.1.9 | General procedure for the synthesis of 3-[1-methyl-3-(phenethylamino)cyclohexyl]phenol (**14**) and 3-[1-methyl-3-(phenylpropylamino)cyclohexyl]phenol (**15**)

To the solution of **13** (197 mg, 964 μmol) in MeOH (4 ml) the corresponding primary amine (1.33 mmol, 1.2 equiv) was added and the resulting mixture was stirred for 5 min, then NaBH_3CN (108 mg, 1.72 mmol, 2 equiv) was added. The reaction mixture was stirred at room temperature for 16 h, then it was concentrated under reduced pressure. The mixture was treated with water and then extracted with EtOAc. The organic extracts were dried over Na_2SO_4 and evaporated. After solvent evaporation, the crude was dissolved in 4 N HCl and purified by flash

chromatography on the reversed-phase column to give compounds **14** or **15** as hydrochloride salts.

3-[1-Methyl-3-(phenethylamino)cyclohexyl]phenol (14) was obtained as a white solid with 83% yield. ^1H NMR (400 MHz, MeOD) δ : 7.36–7.31 (m, 2H), 7.27 (dt, $J = 8.3, 2.2$ Hz, 3H), 7.17 (t, $J = 7.9$ Hz, 1H), 6.85 (ddd, $J = 7.9, 2.0, 0.9$ Hz, 1H), 6.81 (t, $J = 2.1$ Hz, 1H), 6.63 (ddd, $J = 8.1, 2.4, 0.9$ Hz, 1H), 3.49 (q, $J = 7.0$ Hz, 1H), 3.28–3.20 (m, 2H), 3.08–2.93 (m, 3H), 2.77–2.68 (m, 1H), 2.39 (d, $J = 10.8$ Hz, 1H), 2.03 (d, $J = 9.4$ Hz, 1H), 1.78–1.72 (m, 1H), 1.55–1.35 (m, 4H), and 1.20 (s, 3H) ppm. ^{13}C NMR (101 MHz, CDCl_3) δ : 156.71, 148.37, 135.94, 129.78, 128.98, 128.64, 127.35, 118.05, 112.78, 111.67, 51.29, 45.36, 42.32, 39.43, 38.46, 35.73, 33.86, 32.67, and 27.88 ppm. LC/MS: m/z 310.7 $[\text{M}]^+$.

3-[1-Methyl-3-((3-phenylpropyl)amino)cyclohexyl]phenol (15) was obtained as a white solid with 79% yield. ^1H NMR (400 MHz, MeOD) δ : 7.30 (dt, $J = 6.8, 1.1$ Hz, 1H), 7.28–7.23 (m, 2H), 7.23–7.12 (m, 3H), 6.87–6.78 (m, 2H), 6.63 (ddd, $J = 8.1, 2.4, 0.9$ Hz, 1H), 3.02–2.95 (m, 2H), 2.95–2.88 (m, 1H), 2.76–2.63 (m, 3H), 2.38 (d, $J = 10.9$ Hz, 1H), 2.03–1.93 (m, 3H), 1.76–1.71 (m, 1H), 1.48–1.28 (m, 5H), and 1.19 (d, $J = 4.6$ Hz, 3H) ppm. ^{13}C NMR (101 MHz, CDCl_3) δ : 156.40, 148.50, 139.70, 129.64, 128.66, 128.32, 126.43, 112.76, 112.32, 51.63, 43.77, 42.15, 39.22, 38.53, 35.69, 34.11, 32.68, 27.83, and 27.73 ppm. LC/MS: m/z 324.6 $[\text{M}]^+$.

4.2 | Biology

4.2.1 | General

Animals

All procedures and experiments were carried out in accordance with European Council directives (609/86 and 63/2010) and in compliance with the animal policies issued by the Italian Ministry of Health and the Ethical Committee for Animal Experiments (CESA, University of Cagliari). All possible efforts were made to minimize animal pain and discomfort and to reduce the number of experimental subjects. Male Sprague Dawley rats (Envigo), weighing 200–250 g were used; they were housed four per cage in standard plastic cages with fir chips bedding in standard conditions (20–21°C, 60% humidity, and a 12-h light cycle) food and water being available ad libitum.

Drugs

$[\text{D-Ala}^2, \text{NMe-Phe}^4, \text{Gly-ol}^5]\text{-enkephalin}$ (DAMGO), $[\text{Tyrosyl-3,5-}^3\text{H}(\text{N})]$ and $5'\text{-O-(3-}^{35}\text{S)] thiotriphosphate}$ (^{35}S]GTPyS) (1250 Ci/mmol), ^3H were purchased from Perkin Elmer Life Sciences, Inc. Guanosine $5'\text{-diphosphate}$ (GDP), and guanosine $5'\text{-O-(3-thiotriphosphate)}$ (GTPyS) were obtained from Sigma/RBI. DAMGO, naloxone was purchased from Merck Life Science S.r.l. For biochemical experiments, all drugs were dissolved in dimethyl sulfoxide (DMSO). The DMSO concentration used in the different assays never exceeded 0.2% (v/v) and had no effects on ^3H DAMGO binding and ^{35}S GTPyS binding assays.

4.2.2 | In vitro binding studies

Tissue preparation

Rats were killed by decapitation and their brains were rapidly removed. Total brains were homogenized in 50 volumes (w/v) of ice-cold 50 mM TRIS-HCl buffer (pH 7.4) using a Polytron homogenizer. The homogenate was centrifuged at 48,000 g for 20 min at 4°C, and the resulting pellet was resuspended in 50 volumes of ice-cold buffer (pH 7.4) and incubated for 45 min at 37°C in a water bath. Then, once more the homogenate was centrifuged at 48,000 g for 20 min at 4°C. The final pellet was frozen at -80°C at least for 18–20 h before use for ^3H]DAMGO binding assay. For MOR-stimulated ^{35}S]GTPyS binding, the rat cortex was dissected and homogenized in a Polytron with 20 volumes of 50 mM Tris-HCl, 3 mM MgCl_2 buffer, containing 1 mM EGTA, pH 7.4. The homogenates were centrifuged twice at 48,000 g at 4°C for 10 min, resuspended in homogenization buffer, and frozen at -80°C until use. The Bradford protein assay²² was used for protein determination using bovine serum albumin as a standard in accordance with the supplier protocol (Bio-Rad).

^3H]DAMGO binding assay in brain membranes

Membrane homogenates from rat total brain membranes (300–400 μg) were incubated for 60 min at 25°C with 1 nM of ^3H]DAMGO in a volume of 2 ml of 50 mM buffer TRIS-HCl, pH 7.4. Nonspecific binding was determined in the presence of 10 μM naloxone. ^3H]DAMGO displacement was performed by using several dilutions (0.01, 0.1, 1, and 10 μM) of cold DAMGO or of compounds **8**, **9**, **10**, **11**, **14**, and **15**. The free ligand was separated from the bound ligand by rapid filtration through Whatman GF/B filters, using a Brandell 30-sample harvester. Filters were washed three times with ice-cold Tris-HCl buffer (pH 7.4). Filter-bound radioactivity was counted in a liquid scintillation counter (Packard Tricarb 2810 TR, Packard), using 3 ml of scintillation fluid (Ultima Gold Packard, MV).

^{35}S]GTPyS binding assay in rat cortical membranes

Membrane homogenates from rat cortical membranes (20 μg) were incubated for 60 min at 30°C with and without various drugs, in a final volume of 1 ml assay buffer (50 mM Tris-HCl, 3 mM MgCl_2 , 0.2 mM EGTA, 100 mM NaCl, pH 7.4) containing 0.05 nM ^{35}S]GTPyS and 30 μM GDP. After incubation, samples were filtered using a Packard Unifilter—GF/B, washed twice with 1 ml of ice-cold 50 mM Tris-HCl, pH 7.4 buffer, and dried for 1 h at 30°C. The radioactivity on the filters was counted in a liquid microplate scintillation counter (TopCount NXT; Packard) using 30 μl of scintillation fluid (Microscint 20; Packard). Nonspecific binding was measured in the presence of 10 μM unlabeled GTPyS. Basal binding was assayed in the absence of agonists and in the presence of GDP. Stimulation by the agonist was defined as a percentage increase above basal levels (i.e., $\{[\text{dpm}(\text{agonist}) - \text{dpm}(\text{no agonist})] / \text{dpm}(\text{no agonist})\} \times 100$). Data are reported as the mean of three to four independent experiments, performed in triplicate.

4.3 | Molecular modeling

The crystal structure of the complex «receptor-BF0 ligand» was used as the scaffold of choice to build the μ -opioid receptor virtual model and derived from 2.80 Å (4DKL) RCSB-PDB. Then, naltrexone has been used to validate our docking protocol. The crystal structures of (*Mus musculus*) MOR in the active form bound to the BU72 agonist (PDB ID, 5C1M) were obtained from the RCSB database at 2.07 Å (5C1M).

In more detail, the crystal structure of the “receptor-BF0 ligand” complex (PDB 4DKL) or “receptor-BU72 ligand” complex (5C1M) were used as a frame of reference and loaded into the Maestro software (Schrödinger Release 2018-3)^[23–28] Subsequently, the protein crystals were prepared virtually through the Schrodinger suite. By using the Protein Preparation Wizard, we assigned bond orders, added hydrogens, created zero-order bonds to metals, created disulfide bonds, and filled-in missing side chains and loops. Ligands were optimized at physiological pH (pH 7.0 \pm 1.0) with the Epik algorithm, generating the het states. Default parameters were used for the optimization of hydrogen-bond assignment (sampling of water orientations and use of pH 7.0). Restrained energy minimization was applied on hydrogens only using the OPLS3e force field. Prepared protein systems were further checked by Ramachandran plots, ensuring there were no steric clashes. A docking grid suitable for the size of the ligands was created and then docked for a comparison with the crystallographic ligand. In detail, to generate receptor grids, (inner box size 10 \times 10 \times 10 Å³, outer box 25 \times 25 \times 25 Å³), BF0 was selected as the grid definition ligand for MOR after eliminating the covalent interactions with the receptor. Default Van der Waals radius scaling parameters (scaling factor of 1, partial charge cutoff of 0.25) were used. Then, for correct validation of the MOR inactive model, the Glide algorithm was used, and the free energy of the crystallographic ligand, naltrexone, and naloxone was optimized by means of the MM-GBSA method. The LigPrep panel was used to prepare the ligands by generating possible states at pH 7.0 \pm 2.0 using Epik methodology and retaining the specified stereochemical properties. All compounds were docked into MOR with the most stringent Glide XP docking mode. In particular, the following parameters were employed: default scaling of Van der Waals radii (scaling factor of 0.80, partial charge cutoff of 0.15), flexible docking, postdocking minimization, and 100% retention of scoring compounds.

ACKNOWLEDGMENTS

The work was supported by a Project from the European Commission under the Call JUST-2017-AG-DRUG SUPPORTING INITIATIVES IN THE FIELD OF DRUGS POLICY, JUST-2017-AG-DRUG (Grant agreement no. 806996-JUSTSO). Open Access Funding provided by Università degli Studi di Cagliari within the CRUI-CARE Agreement.

CONFLICTS OF INTEREST

The authors declare no conflicts of interest.

AUTHOR CONTRIBUTIONS

Graziella Tocco: Conceptualization, supervision, validation, writing—original draft, writing—review, and editing. **M. Paola Castelli:**

Investigation, validation, writing—review, and editing. **Antonio Laus:** investigation, visualization, formal analysis. **Maksims Vanejevs and Anastasija Ture:** investigation, visualization. **Rafaela Mostallino:** investigation. **Nicholas Pintori:** formal analysis. **Maria Antonietta De Luca and Gaetano Di Chiara:** writing—review and editing, funding acquisition. All authors have given approval for the final version of the manuscript.

ORCID

Graziella Tocco  <https://orcid.org/0000-0003-0081-5704>

Maria Antonietta De Luca  <https://orcid.org/0000-0002-2647-4859>

M. Paola Castelli  <https://orcid.org/0000-0003-3249-4706>

REFERENCES

- [1] M. García, V. Llorente, L. Garriga, U. Christmann, S. Rodríguez-Esrich, M. Virgili, B. Fernández, M. Bordas, E. Ayet, J. Burgueño, M. Pujol, A. Dordal, E. Portillo-Salido, G. Gris, J. M. Vela, C. Almansa, *J. Med. Chem.* **2021**, 64, 10139. <https://doi.org/10.1021/acs.jmedchem.1c00417>
- [2] A. J. Goodman, B. Le Bourdonnec, R. E. Dolle, *ChemMedChem* **2007**, 2, 1552. <https://doi.org/10.1002/cmdc.200700143>
- [3] D. M. Zimmerman, J. D. Leander, B. E. Cantrell, J. K. Reel, J. Snoddy, L. G. Mendelsohn, B. G. Johnson, C. H. Mitch, *J. Med. Chem.* **1993**, 36, 2833. <https://doi.org/10.1021/jm00072a001>
- [4] F. I. Carroll, R. E. Dolle, *ChemMedChem* **2014**, 9, 1638. <https://doi.org/10.1002/cmdc.201402142>
- [5] F. I. Carroll, J. P. Cueva, J. B. Thomas, S. W. Mascarella, S. P. Runyon, H. A. Navarro, *ACS Med. Chem. Lett.* **2010**, 1, 365. <https://doi.org/10.1021/ml100126b>
- [6] D. M. Zimmerman, R. Nickander, J. S. Horng, D. T. Wong, *Nature* **1978**, 275(5678), 332. <https://doi.org/10.1038/275332a0>
- [7] C. H. Mitch, J. D. Leander, L. G. Mendelsohn, W. N. Shaw, D. T. Wong, B. E. Cantrell, B. G. Johnson, J. K. Reel, J. D. Snoddy, A. E. Takemori, D. M. Zimmerman, *J. Med. Chem.* **1993**, 36, 2842. <https://doi.org/10.1021/jm00072a002>
- [8] A. Hashimoto, A. E. Jacobson, R. B. Rothman, C. M. Dersch, C. George, J. L. Flippen-Anderson, K. C. Rice, *Bioorg. Med. Chem.* **2002**, 10, 3319. [https://doi.org/10.1016/s0968-0896\(02\)00219-5](https://doi.org/10.1016/s0968-0896(02)00219-5)
- [9] I. J. Kim, C. M. Dersch, R. B. Rothman, A. E. Jacobson, K. C. Rice, *Bioorg. Med. Chem.* **2004**, 12, 4543. <https://doi.org/10.1016/j.bmc.2004.05.038>
- [10] K. Cheng, Y. S. Lee, R. B. Rothman, C. M. Dersch, R. W. Bittman, A. E. Jacobson, K. C. Rice, *J. Med. Chem.* **2011**, 54, 957. <https://doi.org/10.1021/jm1011676>
- [11] C. M. Kormos, J. P. Cueva, M. G. Gichinga, S. P. Runyon, J. B. Thomas, L. E. Brieady, S. W. Mascarella, B. P. Gilmour, H. A. Navarro, F. I. Carroll, *J. Med. Chem.* **2014**, 57, 3140. <https://doi.org/10.1021/jm500184j>
- [12] M. S. Kharasch, P. O. Tawney, *J. Am. Chem. Soc.* **1941**, 63, 2308. <https://doi.org/10.1021/ja01854a005>
- [13] C. Harrison, J. R. Traynor, *Life Sci.* **2003**, 74, 489. <https://doi.org/10.1016/j.lfs.2003.07.005>
- [14] R. A. Friesner, J. L. Banks, R. B. Murphy, T. A. Halgren, J. J. Klicic, D. T. Mainz, M. P. Repasky, E. H. Knoll, D. E. Shaw, M. Shelley, J. K. Perry, P. Francis, P. S. Shenkin, *J. Med. Chem.* **2004**, 47, 1739.
- [15] R. A. Friesner, R. B. Murphy, M. P. Repasky, L. L. Frye, J. R. Greenwood, T. A. Halgren, P. C. Sanschagrin, D. T. Mainz, *J. Med. Chem.* **2006**, 49, 6177. <https://doi.org/10.1021/jm0306430>

- [16] C. R. Ellis, N. L. Kruhlak, M. T. Kim, E. G. Hawkins, L. Stavitskaya, *PLoS One* **2018**, 13, e0197734. <https://doi.org/10.1371/journal.pone.0197734>
- [17] M. A. Lill, J. J. Thompson, *J. Chem. Inf. Model.* **2011**, 51, 2680. <https://doi.org/10.1021/ci200191m>
- [18] H. K. Srivastava, G. N. Sastry, *J. Chem. Inf. Model.* **2012**, 52, 3088. <https://doi.org/10.1021/ci300385h>
- [19] G. L. Warren, C. W. Andrews, A. M. Capelli, B. Clarke, J. LaLonde, M. H. Lambert, M. Lindvall, N. Nevins, S. F. Semus, S. Senger, G. Tedesco, I. D. Wall, J. M. Woolven, C. E. Peishoff, M. S. Head, *J. Med. Chem.* **2006**, 49, 5912. <https://doi.org/10.1021/jm050362n>
- [20] P. Ferrara, H. Gohlke, D. J. Price, G. Klebe, C. L. Brooks III, *J. Med. Chem.* **2004**, 47, 3032. <https://doi.org/10.1021/jm030489h>
- [21] P. Srivani, E. Srinivas, R. Raghu, G. N. Sastry, *J. Mol. Graph. Model.* **2007**, 26, 378. <https://doi.org/10.1016/j.jmgm.2007.01.007>
- [22] M. M. Bradford, *Anal. Biochem.* **1976**, 72, 248. <https://doi.org/10.1006/abio.1976.9999>
- [23] X. Peng, B. I. Knapp, J. M. Bidlack, J. L. Neumeyer, *J. Med. Chem.* **2007**, 50(9), 2254. <https://doi.org/10.1021/jm061327z>
- [24] W. Huang, A. Manglik, A. J. Venkatakrishnan, T. Laeremans, E. N. Feinberg, A. L. Sanborn, H. E. Kato, K. E. Livingston, T. S. Thorsen, R. C. Kling, S. Granier, P. Gmeine, S. M. Husbands, J. R. Traynor, W. I. Weis, J. Steyaert, R. O. Dror, B. K. Kobilka, *Nature* **2015**, 524, 315. <https://doi.org/10.1038/nature14886>
- [25] A. Koehl, H. Hu, S. Maeda, Y. Zhang, Q. Qu, J. M. Paggi, N. R. Latorraca, D. Hilger, R. Dawson, H. Matile, G. Schertler, S. Granier, W. I. Weis, R. O. Dror, A. Manglik, G. Skiniotis, B. K. Kobilka, *Nature* **2018**, 558, 547. <https://doi.org/10.1038/s41586-018-0219-7>
- [26] Schrödinger Release 2018-3: Maestro, Schrödinger, LLC, New York, NY, **2018**.
- [27] G. M. Sastry, M. Adzhigirey, T. Day, R. Annabhimoju, W. Sherman, *J. Comput. Aided. Mol. Des.* **2013**, 27, 221. <https://doi.org/10.1007/s10822-013-9644-8>
- [28] Schrödinger Release 2018-3: Protein Preparation Wizard; Epik, Schrödinger, LLC, New York, NY, 2018; Impact, Schrödinger, LLC, New York, NY; Prime, Schrödinger, LLC, New York, NY, **2018**.

SUPPORTING INFORMATION

Additional supporting information can be found online in the Supporting Information section at the end of this article.

How to cite this article: G. Tocco, A. Laus, M. Vanejevs, A. Ture, R. Mostallino, N. Pintori, M. A. De Luca, M. P. Castelli, G. Di Chiara, *Arch. Pharm.* **2022**, e2200432. <https://doi.org/10.1002/ardp.202200432>